

Unmasking damped Ly α absorbing galaxies at $z < 1$

Hsiao-Wen Chen¹†

¹Center for Space Research, Massachusetts Institute of Technology,
Cambridge, MA 02139, USA. E-mail: hchen@space.mit.edu

Abstract. I review current results from searching for galaxies giving rise to damped Ly α absorbers (DLAs) at $z < 1$. Using 14 confirmed DLA galaxies, I further show that intermediate-redshift galaxies possess a large HI envelope out to $24 - 30 h^{-1}$ kpc in radius. The photometric and spectral properties of these galaxies confirm that DLA galaxies are drawn from the typical field population, and not from a separate population of low surface brightness or dwarf galaxies. The spatial distribution of metals in the cold ISM of intermediate-redshift galaxies is characterised by a radial gradient of -0.041 ± 0.012 dex per kiloparsec (or equivalently a scale length of $10.6 h^{-1}$ kpc) to $30 h^{-1}$ kpc radius based on an ensemble of six galaxy-DLA pairs. Adopting this abundance gradient and known $N(\text{HI})$ profiles of nearby galaxies, I show that the observed low metal content of the DLA population can arise naturally as a combination of gas cross-section selection and metallicity gradients commonly observed in local disk galaxies.

1. Introduction

Damped Ly α absorbers (DLAs) probe neutral gas regions commonly seen in nearby galaxies (with HI column density $N(\text{HI}) \geq 2 \times 10^{20} \text{ cm}^{-2}$), and therefore represent potential hosts for star formation at high redshift. In principle, galaxies selected by association with DLAs form a unique sample for studying the galaxy population at high redshift, because these galaxies are selected uniformly based on known neutral gas content, rather than optical brightness or colour. Optical spectroscopic surveys for DLAs have demonstrated that DLAs dominate the mass density of neutral gas in the Universe and that they contain roughly enough gas at $z = 3.5$ to form the bulk of the stars in present-day galaxies (Storrie-Lombardi & Wolfe 2000; Péroux *et al.* 2002; Prochaska & Herbert-Fort 2004). But chemical abundance analyses of DLAs at redshift $z < 1.6$ yield sub-Solar metallicities in the neutral gaseous clouds (Pettini *et al.* 1999; Prochaska *et al.* 2003), suggesting that even at low redshift they do not trace the bulk of star formation and are likely to represent a biased sample of galaxies. Because metallicity depends on morphological type and galactocentric distance, it is impossible to understand the origin of DLAs without first identifying the absorbing galaxies.

Identifying optical counterparts of the DLAs is a challenging task, because these galaxies are faint and located at small projected distances to the background bright QSOs (as implied by the intrinsic high column density of the absorbers). Le Brun *et al.* (1997) reported candidate absorbing galaxies toward seven QSO lines of sight with known DLAs based on high spatial resolution HST/WFPC2 images. These galaxies exhibit a wide range in morphological types, from luminous spiral galaxies, to compact objects, and to low surface brightness galaxies. In two fields, they also identify possible groups of galaxies that are associated with the DLAs. In contrast, Rao *et al.* (2003) collected a sample of

† Hubble Fellow.

Table 1. Summary of confirmed DLA galaxies at $z < 1$

QSO (1)	z_{QSO} (2)	z_{DLA} (3)	$\log N(\text{HI})$ (4)	$\Delta\theta$ ($''$) (5)	$\rho \times h^a$ (kpc) (6)	AB (7)	$M_{AB(B)}^b$ $-5 \log h$ (8)	Morphology (9)
TON 1480	0.614	0.0036	20.34	114.0	5.94	$B = 11.5$	-18.7	S0
HS1543+5921	0.807	0.009	20.35	2.4	0.31	$R = 16.5$	-15.3	LSB
PKS0439-433	0.593	0.101	19.85	3.9	5.13	$I = 17.2$	-19.6	disk
Q0738+313	0.635	0.2212	20.90	5.7	14.23	$I = 20.9$	-17.7	compact
Q0809+483	0.871	0.4368	20.80	1.5	5.9	$R = 19.9$	-20.3	disk
B2 0827+243	0.939	0.525	20.30	5.8	25.42	$R = 21.0$	-20.0	disk
PKS1629+120	1.795	0.532	20.70	3.0	13.24	$R = 21.6$	-19.2	disk
LBQ50058+0155	1.954	0.613	20.08	1.2	5.67	$R = 23.7$	-17.6	disk
HE1122-1649	2.400	0.681	20.45	3.6	17.66	$I = 22.4$	-18.8	compact
FBQS 0051+0041	1.190	0.740	20.40	3.3	16.87	$I = 22.4$	-18.6	compact
EX0302-2223	1.400	1.001	20.36	3.3	18.65	$R = 23.2$	-19.3	Irr
PKS 1127-145	1.187	0.313	21.71	3.8	12.2	$R = 22.4$	-16.8	Irr
				3.8	12.2	22.1	-17.4	compact
				9.8	31.5	19.1	-20.1	disk
				17.5	56.2	18.9	-20.3	disk
AO0235+164	0.940	0.524	21.70	2.1	9.4	$I = 20.2$	-20.3	compact
				6.4	28.0	$I = 20.9$	-19.7	compact
FBQS 1137+3907	1.020	0.719	21.10	2.5	12.6	$K = 21.4$	-18.8	compact
				1.5	7.6	$K = 21.7$	-18.5	Irr

a. A Λ cosmology, $\Omega_M = 0.3$ and $\Omega_\Lambda = 0.7$ with $h = H_0/(100 \text{ km s}^{-1} \text{ Mpc}^{-1})$ is adopted throughout.
 b. $M_{AB(B)} - 5 \log h = -19.6$ (Ellis *et al.* 1996).

Table 2. Summary of candidate DLA galaxies at $z < 1$

QSO (1)	z_{QSO} (2)	z_{DLA} (3)	$\log N(\text{HI})$ (4)	$\Delta\theta$ ($''$) (5)	$\rho \times h$ (kpc) (6)	AB (7)	$M_{AB(B)}^b$ $-5 \log h$ (8)	References (9)
Q0738+313	0.635	0.0912	21.18	$K > 17.8$	> -18.8	1,2
PKS0952+179	1.472	0.2390	21.32	3
PKS1229-021	1.038	0.3950	20.60	1.4	≈ 5.2	$R = 22.1$	≈ -18.4	4
Q1209+107	2.191	0.6295	20.48	1.6	≈ 7.7	$R = 21.6$	≈ -20.5	5
PKS1622+23	0.927	0.6563	20.36	$R > 24.5$	> -16.9	6
Q1328+307	0.849	0.692	21.30	2.0	≈ 10	$I = 22.1$	<i>approx</i> -19.3	5
PKS0454+039	1.345	0.8596	20.76	0.8	≈ 4.3	$R = 24.2$	≈ -19.0	4,5

1. Turnshek *et al.* (2001); 2. Cohen (2001); 3. Rao *et al.* (2003); 4. Steidel *et al.* (1994); 5. Le Brun *et al.* (1997); 6. Steidel *et al.* (1997).

14 candidate or confirmed DLA galaxies, and argued that low-luminosity dwarf galaxies dominate the DLA galaxy population with $\approx 50\%$ of the DLAs originating in galaxies of luminosity $L \leq 0.25 L_*$.

Extensive searches in the past decade have resulted in a significant increase in the number of confirmed DLA galaxies. Of all the 23 DLA systems known at $z \leq 1$, 14 have been identified with their host galaxies using spectroscopic redshift techniques (see section 2 for a complete list). Here I first review current results from searching for $z < 1$ DLA galaxies. Then I compare the optical properties of the absorbing galaxies, such as B -band luminosity and stellar content, with known properties of the absorbers such as $N(\text{HI})$ and metallicity.

2. A sample of DLA galaxies at $z < 1$

A list of 14 DLA galaxies confirmed using either spectroscopic or photometric redshift techniques is presented in Table 1 (see also Chen & Lanzetta 2003 for a list of references and Lacy *et al.* 2003 for new additions). It is interesting to note that the three highest- $N(\text{HI})$ DLAs are found to be associated with groups of galaxies within a small projected distance (the last three DLAs in Table 1). In addition, the DLAs toward TON 1480 and HS1543+5921 were discovered in targeted searches of DLAs, with a prior knowledge of the presence of a foreground galaxy within a small radius from the sight-line, while the rest of the absorbers are identified in a survey of random QSO sight-lines.

Additional efforts have been made to search for the absorbing galaxies of the seven DLAs listed in Table 2. Candidate galaxies are found for the DLAs toward PKS0952+179,

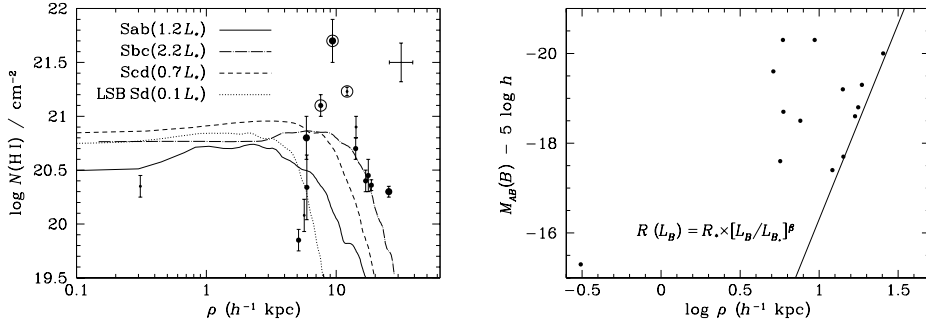


Figure 1. Left: $N(\text{HI})$ distribution versus galaxy impact parameter ρ from 14 DLA galaxies (points), compared to the mean HI profiles of nearby galaxies of different morphological type and intrinsic luminosity (curves). Right: The distribution of B -band absolute magnitude versus ρ for the 14 galaxies. The solid line shows the best-fit scaling relation that describes the apparent envelope stretching to larger ρ at brighter $M_{AB}(B)$.

PKS1229–021, Q1209+107, Q1328+307, and PKS0454+039 based on their close proximity to the QSO sight-lines, while no candidates are found for the DLAs toward Q0738+313 and PKS1622+23 after extensive surveys. No search effort is known for the DLAs at $z_{\text{DLA}} = 0.6847$ toward Q0218+357 and at $z_{\text{DLA}} = 0.394$ toward Q0248+43.

The collection of 14 confirmed DLA galaxies represents the first large DLA-selected galaxy sample, which allows us (1) to determine the neutral gas cross-section of intermediate-redshift galaxies; (2) to establish an empirical correlation between the kinematics and metallicity of the absorbers and those of the absorbing galaxies; and (3) to study the disk population at intermediate redshift using galaxies selected uniformly based on known neutral gas content, rather than optical brightness or colour.

3. The HI extent of intermediate-redshift galaxies

Fig. 1 shows $N(\text{HI})$ versus ρ for the 14 galaxy and DLA pairs in the left panel. Mean HI surface density profiles measured from 21-cm observations of nearby galaxies of different morphological type and intrinsic luminosity are presented in different curves (the mean HI profiles for Sab, Sbc, and Scd galaxies were digitised from Cayatte *et al.* 1994; the curve for LSB Sd was provided by Uson & Matthews 2003). The scatter of $N(\text{HI})$ at the Holmberg radii and the scatter of the neutral gaseous extent at $N(\text{HI}) = 10^{20} \text{ cm}^{-2}$ from 21-cm data for Sd-type galaxies are marked by the error bar in the upper-right corner (Cayatte *et al.* 1994). The three DLAs found in groups of galaxies are marked in circles. The size of the points indicates the intrinsic brightness of the galaxies: $M_{AB}(B) - 5 \log h \leq -19.6$ (large), $-19.6 < M_{AB}(B) - 5 \log h \leq -18$ (medium), and $M_{AB}(B) - 5 \log h > -18$ (small). Despite the apparent large scatter in the $N(\text{HI})$ distribution, we see two interesting features. First, the $N(\text{HI})$ in DLAs is not grossly different from the mean HI distribution of nearby galaxies, although we note that measurements obtained in 21-cm observations are smoothed over a finite beam size. Second, while the HI extent of these intermediate-redshift galaxies appears to be comparable to that of nearby galaxies, most DLAs tend to lie at slightly larger radii from the absorbing galaxies for a given $N(\text{HI})$.

The extent of neutral gas around intermediate-redshift galaxies may be quantified based on the distribution of $M_{AB}(B)$ versus ρ of known galaxy-DLA pairs. The right panel of Fig. 1 presents the $M_{AB}(B)$ versus ρ distribution for 14 galaxy-DLA pairs.

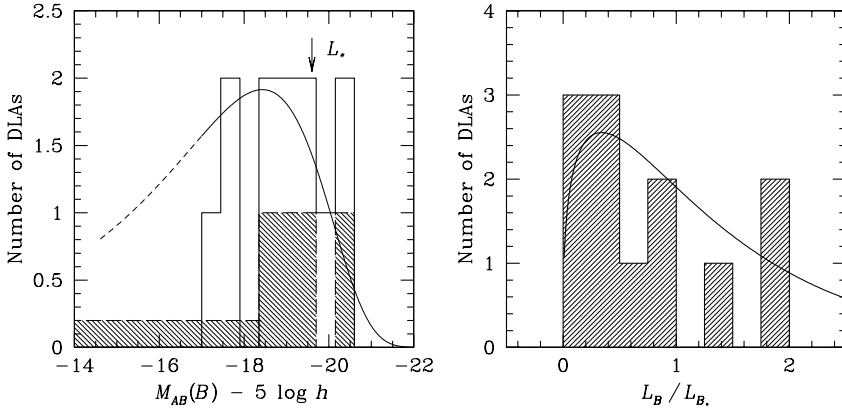


Figure 2. Luminosity distribution of DLA galaxies, in comparison to the prediction (the solid curve) from adopting a Schechter luminosity function, characterised by $M_{AB*}(B) = -19.6$ and $\alpha = -1.4$, and the scaling relation (Eq. 3.1). The model is normalised to match the total number of DLA galaxies in the homogeneous sample. The dashed curve indicates the expected number of DLAs produced by these fainter galaxies if their neutral gas cross section were to be characterised by the same scaling relation of the more luminous ones. We present the distribution in absolute magnitudes in the left panel and in luminosity in the right panel. The solid histogram in both panels is for DLA galaxies with confirmed redshift measurements. The dashed histogram in the left panel is for candidate DLA galaxies only.

It shows that the data points are enclosed in an envelope that stretches to larger ρ at brighter $M_{AB}(B)$, indicating a finite size for the underlying HI disks. Chen & Lanzetta (2003) adopted a power-law model to characterise this envelope

$$\frac{R}{R_*} = \left(\frac{L_B}{L_{B*}} \right)^\beta, \tag{3.1}$$

and found $R_* = 24 - 30 h^{-1}$ kpc and $\beta = 0.26 - 0.29$ for $M_{AB*}(B) - 5 \log h = -19.6$ (Ellis *et al.* 1996).

4. Photometric properties of the DLA galaxies

A comparison of the luminosity distribution of the DLA galaxies and models derived from adopting the scaling relation of Eq. 3.1 and a known galaxy luminosity function allows us to determine how galaxies of different intrinsic luminosity contribute to the total neutral gas cross section. The results are presented in Fig. 2 for 12 confirmed DLA galaxies selected from random lines of sight (excluding the two systems toward TON 1480 and HS1543+5921; see § 2). Fig. 2 shows that the observed luminosity distribution of the DLA galaxies agrees well with what is expected from the field galaxy population, if all field galaxies possess an extended HI envelope described by Eq. 3.1. In addition, it shows that $\approx 30\%$ of the DLAs originate in dwarf galaxies of $L_B \leq 0.25 L_{B*}$, $\approx 50\%$ of the DLAs originate in sub- L_* galaxies of $0.25 L_{B*} \leq L_B \leq L_{B*}$, and $\approx 20\%$ of the DLAs originate in super- L_* galaxies of $L_B \geq L_{B*}$. Including candidate DLA galaxies listed in Table 2 does not alter the luminosity distribution.

High spatial resolution images of low-redshift DLA galaxies available in the literature already display a wide range of morphological types among galaxies that are associated with DLAs (Le Brun *et al.* 1997; Turnshek *et al.* 2001; Chen & Lanzetta 2003). Fig. 3

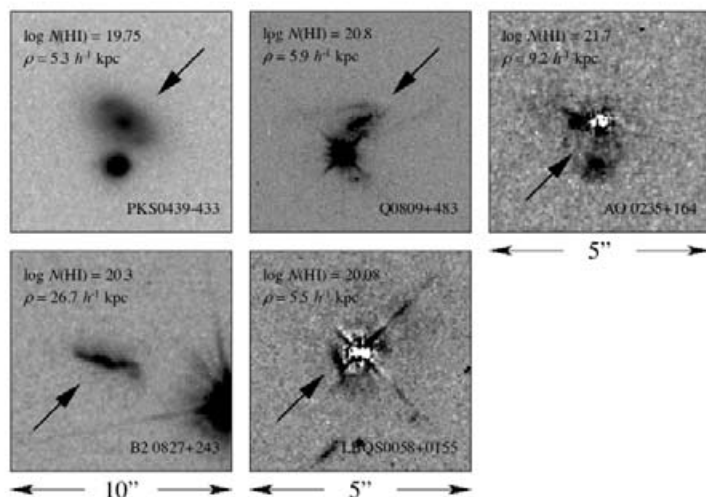


Figure 3. Direct images of five DLA galaxies at $z < 0.65$, showing a range of morphologies. The images are 10 arc-sec on a side for the fields toward PKS0439–433 and B2 0827+243 and 5 arc-sec for the rest. Field orientation is arbitrary. The light from the background QSOs toward AO 0235+164 and LBQS0058+019 have been subtracted to bring out the faint features of the absorbing galaxies (Chen *et al.* 2004).

presents individual images of five additional DLAs for which moderate resolution spectra of the absorbing galaxies are available. The summary in Table 1 indicates that of all the 14 confirmed DLA galaxies, 43% are disk dominated, 22% are bulge dominated, 14% are irregular, and 21% are in galaxy groups, confirming that DLAs originate in galaxies of different morphologies and are associated with a variety of galaxy environments.

5. Abundance profiles of the DLA galaxies

To investigate whether or not metallicity gradients exist in intermediate-redshift galaxies, Chen *et al.* (2005) collected a sample of six galaxy-DLA pairs for which Fe abundance measurements in the neutral gas are available. The results are presented in Fig. 4, where a declining trend of metallicities in neutral gaseous clouds with increasing impact parameter is apparent. The data are best described by a simple correlation,

$$Z(\rho) = (0.02 \pm 0.20) - (0.041 \pm 0.012) \frac{\rho}{(\text{kpc})}, \quad (5.1)$$

where Z is the measured Fe abundance normalised to Solar on a logarithmic scale. The best-fit slope $-(0.041 \pm 0.012)$ corresponds to a scale length of $10.6 h^{-1}$ kpc, in good agreement with the observed oxygen abundance gradient of M101 (Kennicutt *et al.* 2003).

Past studies show consistently that the mean metallicities observed in DLA systems are only a tenth of the Solar values at all redshifts that have been studied (e.g. Pettini *et al.* 1999; Prochaska *et al.* 2003). Chen *et al.* (2005) demonstrate that adopting the metallicity gradient from Eq. 5.1 together with a gas cross-section selection yields a mean metallicity that is consistent with observations at $z < 1.6$. This result confirms that at least at low redshift the low metal content of DLA systems does not rule out the possibility that the DLA population trace the field galaxy population. Whether or not

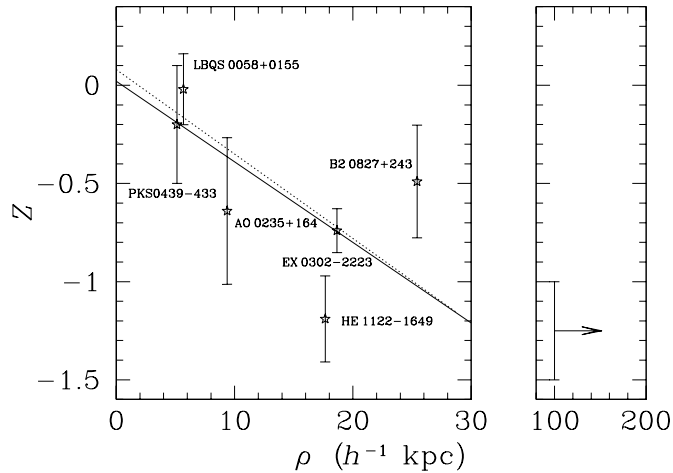


Figure 4. Metallicity of neutral gas Z versus galaxy impact parameter ρ with $Z = 0$ indicating Solar metallicity. Open stars are derived metal abundances after corrections for dust depletion with corresponding $1\text{-}\sigma$ measurement errors. The solid line represents the best-fit correlation between Z and ρ , in comparison to the observed gradient of the H II region oxygen abundance in M101 (dotted line; Kennicutt *et al.* 2003). The intergalactic medium metallicity estimated based on five $z < 0.5$ Ly α absorbers with $N(\text{HI}) = 10^{14-16} \text{ cm}^{-2}$ (see Chen *et al.* 2005) is placed at a distance beyond $\rho = 100 h^{-1} \text{ kpc}$ in the right panel.

the same scenario can be applied to the DLA systems at higher redshifts awaits a large sample of $z > 1.6$ DLA galaxies to be found.

Acknowledgements

This research was supported in part by NASA through a Hubble Fellowship grant HF-01147.01A from STScI, which is operated by the AURA under contract NAS5-26555.

References

- Cayatte, V., Kotanyi, C., Balkowski, C., van Gorkom, J. H., 1994, *AJ*, 107, 1003
 Chen, H.-W., Lanzetta, K. M., 2003, *ApJ*, 597, 706
 Chen, H.-W., Kennicutt, R. C. Jr., Rauch, M., 2005, *ApJ*, 620, 703
 Cohen, J. G., 2001, *AJ*, 121, 1275
 Ellis, R. S., *et al.*, 1996, *MNRAS*, 280, 235 5
 Kennicutt, R. C. Jr., Bresolin, F., Garnett, D. R., 2003, *ApJ*, 591, 801
 Le Brun, F., Bergeron, J., Boissé, P., & Deharveng, J. M., 1997, *A&A*, 321, 733
 Péroux, C., *et al.*, 2002, *Ap&SS*, 281, 543
 Pettini, M., Ellison, S. L., Steidel, C. C., & Bowen, D. V., 1999, *ApJ*, 510, 576
 Prochaska, J. X., *et al.*, 2003, *ApJS*, 147, 227
 Prochaska, J. X., & Herbert-Fort, S., 2004, *PASP*, 116, 622
 Rao, S. M., *et al.*, 2003, *ApJ*, 595, 94
 Steidel, C. C., *et al.*, 1997, *ApJ*, 480, 568
 Steidel, C. C., Pettini, M., Dickinson, M., & Persson, S. E., 1994, *AJ*, 108, 2046
 Storrie-Lombardi, L. J., Wolfe, A. M., 2000, *ApJ*, 543, 552
 Turnshek, D. A., *et al.*, 2001, *ApJ*, 553, 288
 Uson, J. M., Matthews, L. D., 2003, *AJ*, 125, 2455